JTTEE5 15:701-707
DOI: 10.1361/105996306X147117
1059-9630/$19.00 © ASM International

Plasma Spray Synthesis from Precursors: Progress, Issues, and Considerations

B.G. Ravi, S. Sampath, R. Gambino, P.S. Devi, and J.B. Parise

(Submitted February 28, 2006; in revised form May 11, 2006)

Precursor plasma spray synthesis is an innovative and rapid method for making functional oxide ceramic coatings by starting from solution precursors and directly producing inorganic films. This emerging method utilizes molecularly mixed precursor liquids, which essentially avoids the handling and selection of powders, opening up new avenues for developing compositionally complex functional oxide coatings. Precursor plasma spray also offers excellent opportunities for exploring the nonequilibrium phase evolution during plasma spraying of multicomponent oxides from inorganic precursors. Although there have been efforts in this area since the 1980s and early 1990s with the goal of synthesizing nanoparticles, only recently has the work progressed in the area of functional systems. At the Center for Thermal Spray Research an integrated investigative strategy has been used to explore the benefits and limits of this synthesis strategy. Water- and alcohol-based sol/solution precursors derived from various chemical synthesis methods were used as feedstocks to deposit thin/thick films of spherical and nanostructured coatings of yttrium aluminum garnet (YAG), yttrium iron garnet, lanthanum strontium manganate and Zr-substituted yttrium titanates, and compositions of Y_2O_3-Al_2O_3 and their microstructural space centered around stoichiometric YAG. A detailed discussion of the salient features of the radiofrequency induction plasma spraying approach, the results obtained in the investigations to develop various functional oxide coatings, and process issues and challenges are presented.

Keywords ceramic coatings, liquid precursor, luminescent coatings, magnetic properties, microstructure, thermal plasma spraying

1. Introduction

Precursor-based synthesis of inorganics has spawned a new era in materials research and has expanded the capabilities for synthesizing compositionally complex multicomponent systems with a desirable homogeneity and high chemical purity (Ref 1, 2). These approaches allow the exploration of compositional/phase space, helping to identify regions of interest for functionality. Systems of general interest include electrodes/electrolytes for solid oxide fuel cells, advanced ferrites and dielectrics for magnetic/electromagnetic applications, novel sensor materials with high sensitivity/selectivity, and composites. Thermal spraying (TS) expands the potential of precursor routes by offering access to thermal excursions with extreme temperature-time profiles, coupled with the capability for the deposition of novel materials in useful coating and thin film forms (Ref 3-11). The precursor TS approach also obviates the need for producing and handling of powders required in conventional TS, and thus allows the rapid assessment of compositions and materials, especially when coupled with combinatorial schemes. Because powders of the more attractive compositions can also be synthesized by precursor routes and deposited through traditional TS, the strategy should ultimately enable faster discovery and insertion of new materials into applications.

Traditional TS utilizes powder feedstock of premixed compositions to produce ceramic coatings. However, when complex multicomponent oxide films are desired, wide-ranging issues associated with composition and phase stability arise and make it difficult to explore the compositional field and its effect on film characteristics. For instance, some of the early work on precursor-based processing was initiated in late 1980s at the State University of New York at Stony Brook as a part of the efforts to produce oxide superconductor films of the Y-Ba-Cu oxide family. The powder-based method indicated preferential CuO vaporization during plasma spraying, pointing to the need for the overcompensation of CuO in the powder. However, to focus in on the chemistry sweet spot required extensive evaluation of a variety of starting powder compositions. The precursor approach allowed a much more rapid method to explore the chemistry field. Since then, a number of studies have been conducted with varying fundamental and applied interests, but new capabilities in solution chemistry, precursor injection, and plasma spray processes have led to renewed interest in this area. The advent of nanotechnology has expanded the field considerably.

This article was originally published in *Building on 100 Years of Success: Proceedings of the 2006 International Thermal Spray Conference* (Seattle, WA), May 15-18, 2006, B.R. Marple, M.M. Hyland, Y.-Ch. Lau, R.S. Lima, and J. Voyer, Ed., ASM International, Materials Park, OH, 2006.

B.G. Ravi, S. Sampath, and **R. Gambino,** Center for Thermal Spray Research, Department of Materials Science and Engineering; **J.B. Parise,** Department of Geosciences and Chemistry, State University of New York, Stony Brook, NY; and **P.S. Devi,** Electroceramics Division, Central Glass and Ceramic Research Institute, Kolkata, India. Contact e-mail: bravi@notes.cc.sunysb.edu.

The TS coupled with precursor solution chemistry allows the exploration of optical, magnetic, and electronic oxides. Furthermore, given the extreme conditions one would anticipate in the formation/stabilization of metastable phases, TS therefore represents a unique synthetic tool for solid-state chemistry.

Multipronged efforts at various institutions during the 1990s witnessed trials of solution/suspension spray. In early trials at the University of Sherbrooke, several materials were tried with some success using axial feed suspension plasma spray (Ref 3, 4). Recently, liquid suspension plasma spraying has been used to make yttria-stabilized zirconia and $LaMnO_3$ perovskite thin film coatings (Ref 5, 6). Here, the inorganic material was introduced in a liquid suspension and did not use any chemical modification that results from precursor decomposition. Combustion chemical vapor deposition (CVD), which is a complementary process using combustion rather than plasma, has been used at Georgia Institute of Technology to synthesize coatings of metals, oxides, and polymer composites (Ref 12).

Non-vapor phase methods such as solution precursor plasma spray, which is based on direct current (dc) plasma, have been developed for synthesizing nanostructured powders and coatings (Ref 7-11). In dc plasma approaches, a precursor solution is injected radially into the plasma. The dc plasma methods have the following issues to consider: contamination of the product by arc erosion of the dc electrodes; reactive gases, when used to affect chemistry, can potentially react with dc electrodes; and external radial injection of feedstock produces less homogeneous thermal processing and reduces material-processing efficiency.

2. Experimental

2.1 Radiofrequency-Precursor Plasma Spray

Recent work at the State University of New York at Stony Brook has focused on radiofrequency induction precursor plasma spray (RFPPS), utilizing molecularly mixed precursor liquids, which were successfully used to deposit thin/thick films of functional oxides (Ref 13-17). The important advantages of RFPPS include: axial feeding of precursor solution/sol into the larger hot zone, which would provide a longer particle residence time; and the electrode-free nature of radiofrequency (RF) plasma, which avoids contamination from the electrodes. The RFPPS offers much greater operational temperature, large temperature gradients, and very short exposure time in the flame, which facilitate the investigation of the opportunities/implications of metastable phases, stoichiometries and microstructures. Our interests in the development of functional oxides from precursors are both science-based (e.g., precursor development, exploratory synthesis, and process understanding/modeling) and technology-based (e.g., property assessment for potential application, identifying key barriers to implementation and perspective paths to overcome the barriers). Systems of particular interest that were studied/developed included large-area luminescence coating, electrodes/electrolytes for solid oxide fuel cells and gas separation membranes, advanced ferrites, and dielectrics for magnetic/electromagnetic applications.

Initial trials involved simple single-phase oxides, for instance by spraying aluminum nitrate or bohemite sol, which resulted in γAl_2O_3 coatings. Crystalline Y_2O_3 coatings were obtained when yttrium nitrate (in water) was sprayed. This encouraging result provided confidence to examine more compositionally complex systems: yttria-stabilized zirconia; pure and doped garnets [i.e., yttrium aluminum garnet (YAG) and yttrium iron garnet (YIG) and Eu-doped garnets], lanthanum strontium manganate (LSM), and Zr-substituted $Y_2Ti_2O_7$ pyrochlores. Although the development of coatings of the above-mentioned functional oxides had varying success, many challenges remain, but healthy and growing interdisciplinary collaborations are promising. This article reviews the progress, critical observations, and challenges in developmental work on Eu-Y_2O_3 (a luminescent material), YAG, YIG, and LSM.

Table 1 Spray parameters used to make YIG coatings

Parameter	Value
Power, kW (EKNA torch)	60 kW
Chamber pressure, kPa	13-16
Plasma swirl gas (argon), slpm	25
Plasma sheath gas (argon/helium), slpm	85/150
Atomized gas	Helium
Feed rate, mL/min	10-30
Substrate-torch distance, mm (TAFA torch/TEKNA torch)	200/250
Traverse speed, cm/s	2.5
Number of passes (preheat/deposit)	4/20

slpm, standard liter per minute
Source: Ref 17

2.2 Precursor Development and Plasma Spraying

Several precursor liquids solution/sol/polymeric complexes were evaluated for different oxide systems. The success of a particular precursor in forming the required phase for a given system mainly depends on the decomposition characteristics of that precursor. Some of the precursors studied include: (a) mixture of nitrates in water/ethanol (solution); (b) mixture of nitrates and metalorganics in isopropanol (hybrid sol); (c) mixed citrate-nitrate solution (polymeric complex); and (d) coprecipitation followed by peptization (gel dispersion in water/ethanol).

Precursor liquids feedstocks were sprayed using RF plasma torches manufactured by both TAFA (model 66; TAFA, Concord, NH) and TEKNA (model PL-100; TEKNA Plasma Systems Inc., Sherbrooke, ON, Canada) under a series of spray conditions (Ref 13-17). For the development of the coatings, the precursor sol/solution was fed to the RF plasma torch and directly gas atomized into the plasma (Ar/He) through an atomizing probe. As an example, the typical spray parameters used to make YIG coatings are shown in Table 1. The substrate holder was designed to enable spraying simultaneously onto substrates at different distances from the torch nozzle. The substrates were moved horizontally during spraying, while the plasma torch was held stationary.

Under optimum spray conditions, the coating thickness depended primarily on the concentration of the sol and the number of passes made. In a typical spray run, about 200 mL of sol was sprayed continuously, which is sufficient for about 20 passes over the substrates ($6 \times 2.5 \times 0.2$ cm). The average time required to develop a coating with a thickness of 80 to 100 μm was ~40s. Repeating the experiment as many as five times ensured the reproducibility of the desired coating composition. The typical

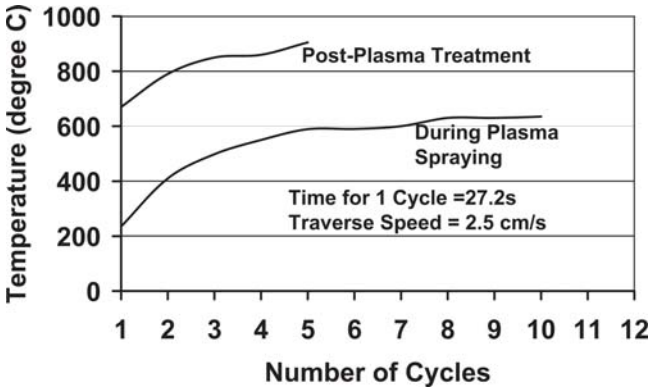

Fig. 1 Temperature profile. The temperature of the substrate was measured using a thermocouple during plasma spraying and post-plasma treatment (heated with plasma flame after spraying).

substrate temperature profile during spraying and after plasma treatment of YAG (Ref 14) is shown in Fig. 1.

3. Discussion

3.1 Eu-Y_2O_3 Luminescent Coatings

The extraordinary chemical stability, luminescent efficiency, and environmental safety makes europium-doped Y_2O_3 phosphors the most promising oxide-based red phosphor known so far. Europium-doped yttrium oxide (Y_2O_3:Eu^{3+}) crystalline coatings (Ref 13) were produced from the mixture of yttrium nitrate hexahydrate, and europium nitrate pentahydrate in water or water/ethanol. The precursor solution was prepared by dissolving yttrium nitrate hexahydrate, $Y(NO_3)_3 \cdot 6H_2O$ Aldrich, St. Louis, MO), europium nitrate pentahydrate, $Eu(NO_3)_3 \cdot 5H_2O$ (Aldrich, 99.9%), in ethanol. The europium ratio was varied from 0.1 to 6 at.% in the system $(Y_{1-x}Eu_x)_2O_3$ to produce these phosphor coatings. The precursor solution was sprayed using the RF plasma torch (TAFA) under a series of spray conditions. Coatings with a thickness of ~60 to 100 μm were developed for use on steel plates and silicon (100) substrates.

In this study for a Y-to-Eu ratio of 98:2, the best luminescent coatings were obtained, and this was the one with a lower amount of europium than the traditional phosphor composition (in traditional red phosphor a Y-to-Eu ratio of 96:4 was mainly used). X-ray diffraction (XRD) analyses on these coatings confirmed that polycrystalline cubic Y_2O_3 phase formed in situ with no impurity phases. The observed photoluminescence (Fig. 2) from these coatings is in all probability due to the highly crystalline nature of the coating combined with the submicron spherical morphology of the grains (Fig. 3).

An energy-dispersive x-ray analysis of the Y_2O_3:Eu^{3+} coating on Si(100) confirmed a uniform distribution of Eu^{3+} among the 0.5 to 5 μm particles. It also confirmed the presence of both Eu and Y on each individual particle. The surface morphology of the film on Si(100) looks coarse and indicates the presence of micron to submicron spherical/pseudospherical particles on the coating, as is evident in Fig. 3. Coatings produced by this method have better thermal stability and superior adhesion, and

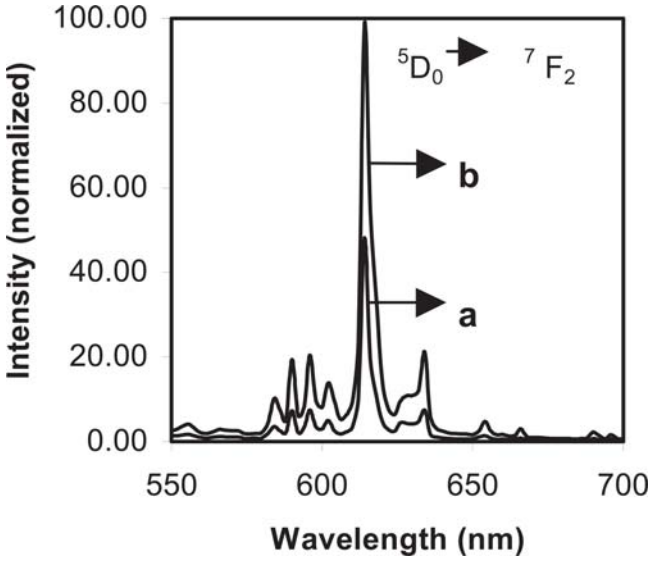

Fig. 2 Photoluminescence (PL) spectra of precursor plasma sprayed Y_2O_3:Eu^{3+} coatings on (a) Si(100) and (b) steel substrates. The excitation wavelength is 260 nm.

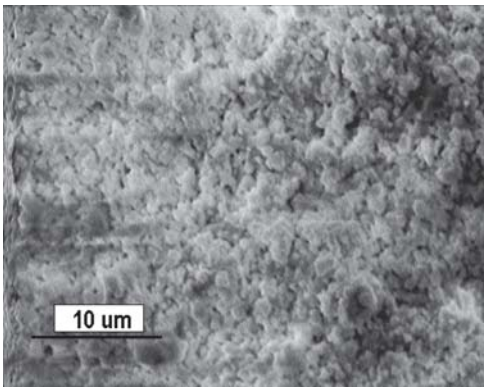

Fig. 3 SEM micrograph of Y_2O_3:Eu^{3+} coating on Si(100) substrate showing the surface image of spherical particles

are expected to offer high contrast due to the higher degree of uniformity and crystallinity over traditional discrete powder coatings.

3.2 Yttrium Aluminum Garnet

Yttrium aluminum garnet ($Y_3Al_5O_{12}$) is a promising high-temperature ceramic and has been used in several applications, such as refractory insulating coatings, optical devices, and phosphors for various display panels, when doped with rare earth elements. Although the superiority of the chemical processes over the traditional ceramic processes is generally recognized, the details of conversion dynamics from the precursors to YAG have remained unclear (Ref 18).

Yttrium aluminum garnet also represents a highly complex oxide with a number of intermediate phases around the congruently melting line compound YAG. Thus, this system represented a unique opportunity to explore the capabilities of the

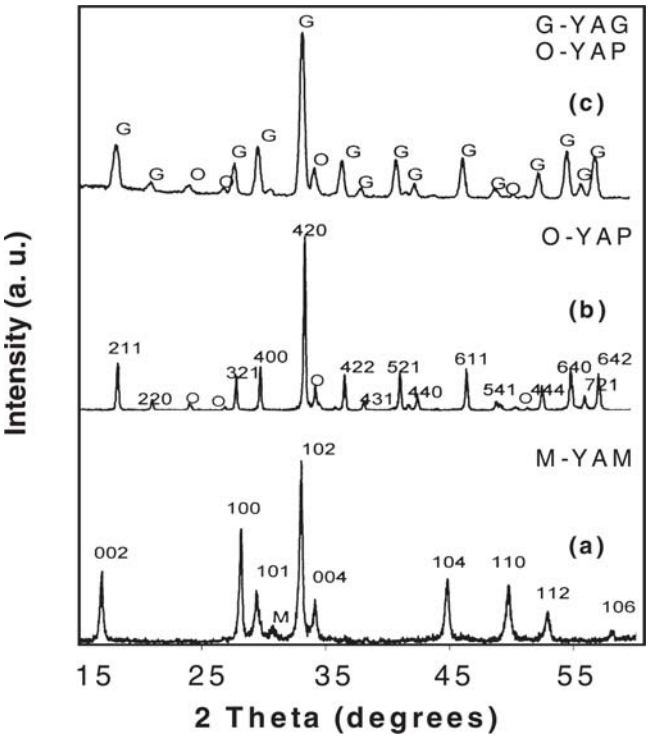

Fig. 4 XRD results of YAG coatings: (a) as-sprayed; (b) treated with plasma for 10 s, wherein the conversion of garnet phase is evident; and (c) sprayed powder calcined at 1250 °C for 6 h

RFPPS process for complex oxides. Much to the authors surprise, it is possible to produce single-phase crystalline coatings of single-phase YAG under certain conditions (Ref 14, 15). The influence of liquid precursors in the form of a solution/sol/polymer complex on the formation of the YAG phase has been investigated.

$Y(NO_3)_3 \cdot 6H_2O$ (Aldrich, 99.9%), $Al(NO_3)_3 \cdot 8H_2O$ (Aldrich, 99.9%), citric acid monohydrate (Alfa Aesar, 99.5%), deionized water, and ethanol were used for the synthesis of YAG. Four precursor feedstocks were used: hybrid sol [a mixture of bohemite (AlO(OH) and yttrium nitrate in water]; a mixture of nitrates in water-ethanol; a mixture of nitrates and citric acid in water; and coprecipitated sol (homogeneous gel obtained from mixture of nitrates dispersed in water). In the case of the mixture of nitrates and citric acid, the YAG precursor solution was prepared by dissolving and mixing the required amount of the metal nitrates in a stoichiometric Y-to-Al ratio of 3:5 in a 1:1 ethanol-deionized water mixture. Citric acid (citrate-to-nitrate ratio of 0.75:0.1) in water was added to the above mixture while stirring. The clear solution obtained was directly sprayed onto substrates.

When a hybrid sol was sprayed through the RF plasma, a metastable hexagonal yttrium aluminate (H-$YAlO_3$) was formed as the major phase (Fig. 4). This phase on further treatment with plasma, was converted to cubic garnet (YAG) as the major phase, with a minor amount of orthorhombic $YAlO_3$ (O-YAP) phase (Ref 14). When a mixture of nitrates and citric acid was sprayed, a mixture of hexagonal $YAlO_3$, O-YAP, yttrium aluminum monoclinic, and YAG was formed, which eventually transformed into YAG after heat treatment at 1000 °C for 6 h (Ref 15). Interestingly, an amorphous phase was formed when a coprecipitated sol was sprayed that completely transformed into YAG after heat treatment at 1000 °C for 30 min. Although these studies point to a potential synthetic strategy, the phase evolution is complex and requires careful parallel studies through phase evolution maps (Ref 18).

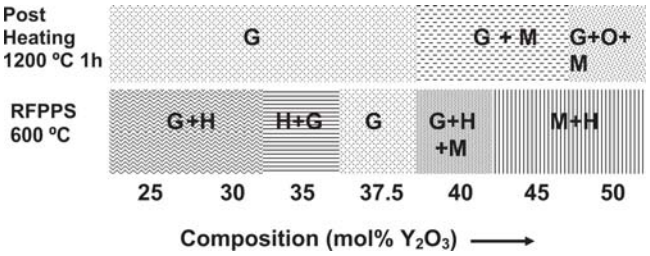

Fig. 5 Phase evolution of Y_2O_3-Al_2O_3 compositions around stoichiometric YAG (37% Y_2O_3) in as-sprayed and post-heat-treated (1200 °C for 1 h) conditions

The overall process of spraying, chemical reaction, and garnet particle formation occurred within 40 s, indicating the simplicity of the process. The RFPPS also presents an opportunity for the production of discrete combinatorial libraries of the functional oxides. Feedstock compositions can be varied by mixing precursors in different proportions while spray conditions were maintained, or vice versa. The authors recently demonstrated the feasibility of this approach to deposit Y_2O_3-Al_2O_3 compositions around stoichiometric YAG. In the discrete combinatorial synthesis approach, mixed nitrate solutions of different compositions having the same final solid concentration were sprayed through RF plasma. Liquid feedstocks of compositions from 25 to 50 Y_2O_3 were sequentially delivered to the injector using a liquid feedstock pump. The shutters placed above the substrate holder and the liquid feedstock pump were programmed in such a way that a particular composition was deposited on the alumina substrate in a chronological order. The crystalline phase was obtained in all the compositions in the as-sprayed condition, and the phase evolution maps of the spray products are presented in Fig. 5.

3.3 Yttrium Iron Garnet

Yttrium iron garnet ($Y_3Fe_5O_{12}$) has attracted much attention in the telecommunications and data storage industries due to their interesting magnetic and magneto-optic properties. Two types of sols made by reverse and regular coprecipitation methods and citrate-nitrate polymeric complex were used as liquid feedstocks (Ref 16, 17).

The YIG precursor sol was prepared by chemical methods using reagent grade nitrates: yttrium nitrate (99.95% purity) and iron (III) nitrate [$Fe(NO_3)_3 \cdot 9H_2O$, 98+% purity] in a 3:5 mol ratio were dissolved in excess of deionized water. Two types of YIG precipitates, namely, REGULAR sol (REG-sol) and REVERSE sol (REV-sol) were prepared. In the case of REG-sol, the mixed nitrate solution turned into a gelatinous mass with the drop-wise addition of ammonia solution (25% ammonium hydroxide, assay 28.0-30.0% NH_3). The gel was washed, filtered out, and redispersed ultrasonically in deionized water. To

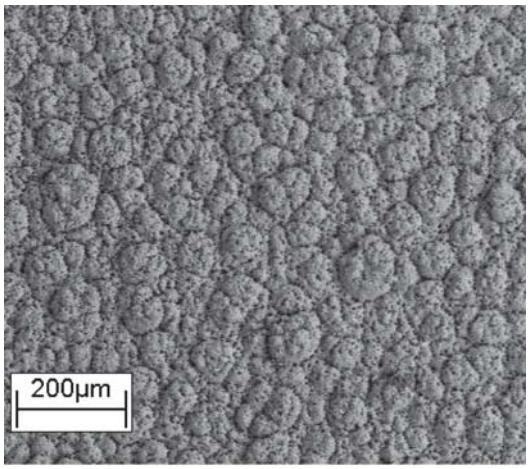

(a)

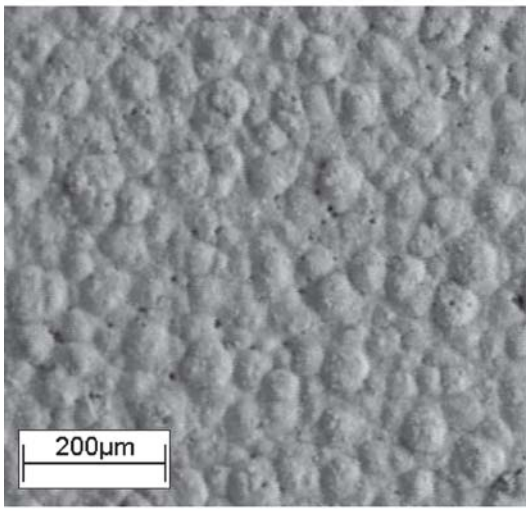

(b)

Fig. 6 SEM micrographs showing the surface features of YIG coatings deposited on alumina substrates using (a) REG-sol and (b) REV-sol

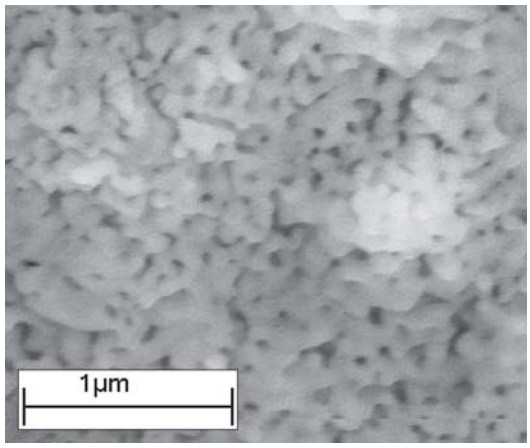

Fig. 7 SEM micrograph showing the morphology of nanostructured grains in a YIG coating annealed at 800 °C for 1 h

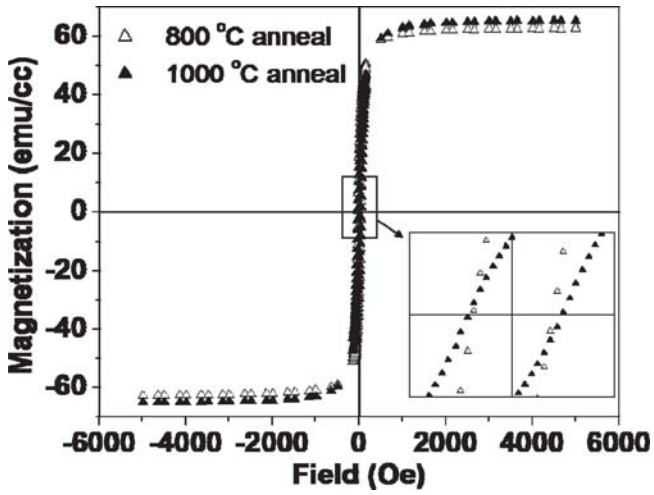

Fig. 8 Room temperature M-H loops of YIG coatings annealed at 800 and 1000 °C for 1 h

prepare a REV-sol, the mixed nitrate solution was added dropwise into a diluted ammonia solution having a pH of 10. In this case, a fresh ammonia solution was constantly added to maintain the pH at 10 throughout the precipitation process. Gel so obtained was then washed and ultrasonically dispersed in deionized water similar to the REG-sol preparation.

An amorphous deposit was obtained in the as-sprayed condition (Ref 17), and a nanostructured coating resulted in annealing treatment at 800 °C for 1 h. The average crystallite size ranged from 32 to 53 nm for coatings annealed at 800 and 1000 °C, respectively. Scanning electron microscopy (SEM) images of surface morphology of REG- and REV-sol-sprayed coatings, in the as-sprayed condition, are shown in Fig. 6. The microstructure of the coating obtained from REV-sol (Fig. 6b) appears denser when compared with that of the coating obtained from REG-sol (Fig. 6a). Figure 7 shows nanostructured grains in the microstructure of a YIG coating annealed at 800 °C; the micrograph also revealed that postannealing treatments promoted growth and the densification of grains.

Magnetic measurements were made using a vibrating sample magnetometer (DMS VSM 1660, ADE Technologies, Westwood, MA), and the hysteresis loops were recorded at room temperature in fields up to 5 kOe. The room temperature magnetization-magnetic field (M-H) curves of YIG coatings annealed at 800 and 1000 °C are compared in Fig. 8. The as-sprayed coating, which was predominantly amorphous, had a low saturation of 2.5 electromagnetic units (emu)/cm^3 and a high coercivity of 163 Oe. Annealing at 800 °C increased the saturation value to 62.8 emu/cm^3 and decreased the coercivity to 31.2 Oe. The increase in the magnetization of the annealed coating can be attributed to the increase in crystallinity and crystallite size with annealing temperature. Coatings annealed at 1000 °C exhibit a saturation magnetization (65.3 emu/cm^3) and a coercivity (37.4 Oe) close to that of the coating annealed at 800 °C. Microstructural and magnetic property studies revealed that better quality coatings can be obtained using a reverse-coprecipitated feedstock sol than a regular coprecipitated one (Ref 17).

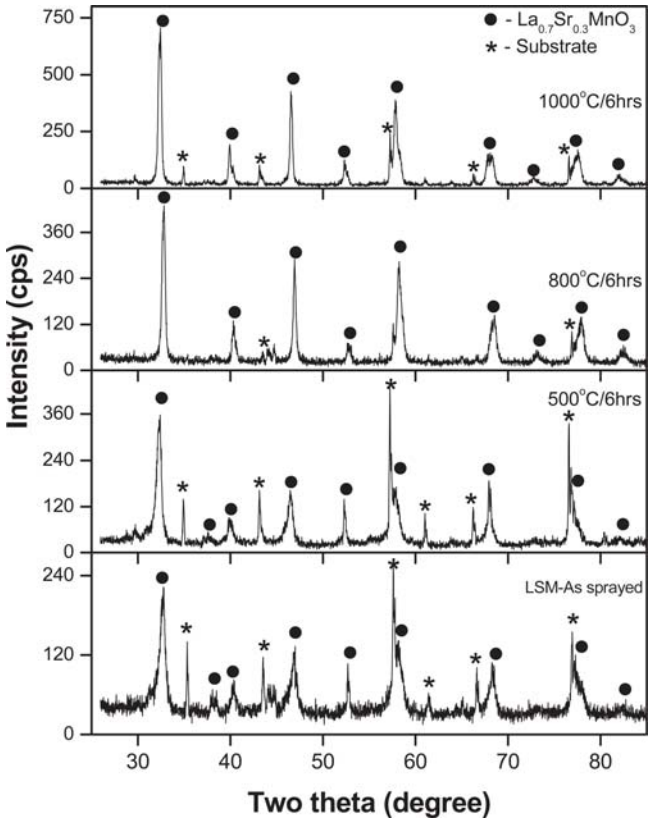

Fig. 9 XRD of RFPPS LSM coatings

3.4 Lanthanum Strontium Manganate

Lanthanum strontium manganate is an established cathode material for solid oxide fuel cells due to its good chemical stability and thermal expansion compatibility with electrolytes. The colossal magnetoresistance effect found in hole-doped (La,Sr) manganates is promising for magnetic sensor applications. Acetate-nitrate as well as citrate-nitrate precursors in water were used as feedstock to form crystalline LSM coatings on alumina and aluminum substrates. A precursor feedstock for a combustion TS was prepared by combining the calculated amounts of metallic nitrates (lanthanum and strontium) and acetate (manganese) in deionized water to ensure the exact stoichiometry of LSM (La-to-Sr-to-Mn ratio 85:15:100). This LSM acetate/nitrate precursor solution was used as the feedstock for a combustion TS using a Terodyn 3000 (Eutectic-Castolin Company, Flushing, NY) oxyacetylene combustion spray gun. A nozzle-substrate distance of 180 mm at gas flows of 30/30 psi, a carrier gas pressure of 22 psi, and a liquid feeder pressure of 8 psi were used. The substrate holder was fixed during spraying, and spraying was performed under stationary conditions for 1 min (Ref 19).

The XRD results (Fig. 9) for as-sprayed and annealed $La_{0.7}Sr_{0.3}MnO_3$ samples essentially shows similar patterns with calculated grain size of 10 nm (as-sprayed) and 23 nm (800 °C) (Ref 19). The typical cross-sectional image of combustion thermal-sprayed LSM coating is shown in Fig. 10.

The early results of magnetocaloric investigations indicate that, although the perovskite phase is represented in the diffraction pattern, magnetic measurements indicate disorder (not surprisingly) within the perovskite phase. The temperature dependence of magnetization of $La_{0.85}Sr_{0.15}MnO_3$ prepared by TS at a measuring field of 0.5 T is shown in Fig. 11. In its as-sprayed state, the $La_{0.85}Sr_{0.15}MnO_3$ sample exhibited at least two magnetic transitions, both with very low magnetizations. This result is strongly suggestive of inhomogeneity/phase separation. The modest annealing treatment of 800 °C for 6 h that was applied to this sample caused the moment to increase dramatically and to exhibit single magnetic-phase behavior. The ferromagnetic response of as-sprayed and annealed films indicated (Fig. 12) that as-sprayed films do not saturate, which again is indicative of two magnetic phases (Ref 19).

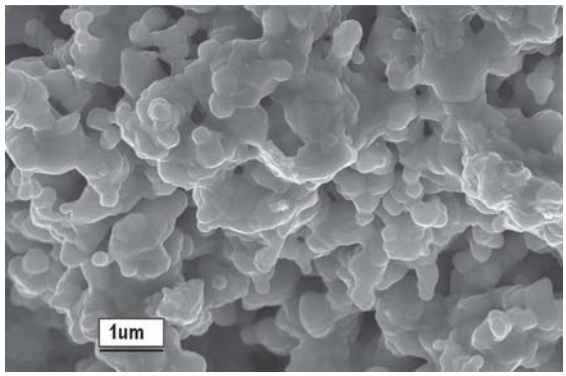

Fig. 10 SEM micrograph showing the cross section of an RFPPS LSM coating

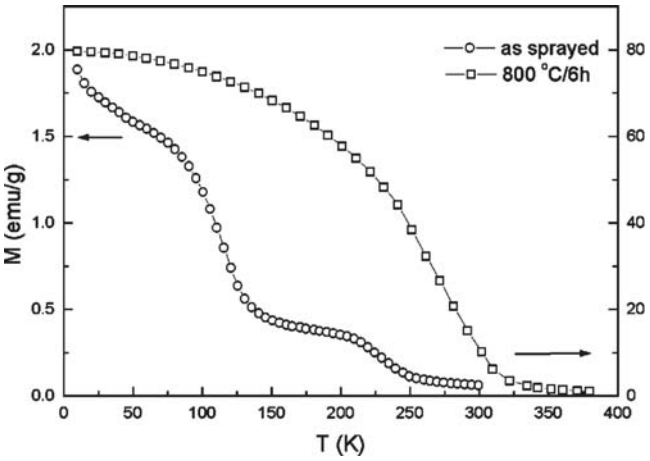

Fig. 11 Temperature dependence of the magnetization of LSM ($La_{0.85}Sr_{0.15}MnO_3$) coatings

4. Summary and Conclusions

This article summarizes the recent progress in the development of and the promising opportunities for RFPPS. The RFPPS is highly promising because its larger heat zone, high temperature, and extremely short exposure time provide opportunities for high-throughput exploratory synthesis and rapid property assessment for targeted application. The RFPPS of systems having

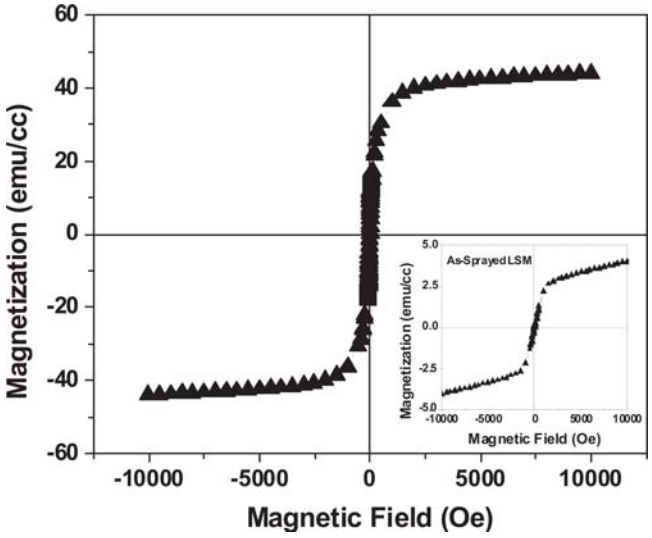

Fig. 12 Room temperature M-H loops of LSM coatings

complex chemistries has been deposited as dense nanostructured coatings in 30 to 40 s. The combination of selective precursor choice and plasma spray parameters can result in thermodynamically stable or metastable materials with unique microstructures. An approach based on a thermodynamic framework and experimentally determined phase evolution map are expected to shed light on our understanding of phase formation.

Acknowledgments

The authors thank J. Margolies and X.Z. Guo for their assistance in processing and analysis. Scientific contributions from Professor Clare Grey, Professor Carlos G.Levi, and Dr. Laura H. Lewis are acknowledged. This research was supported by the Materials Research Science & Engineering Center (MRSEC) program of the National Science Foundation under award DMR-0080021.

References

1. F.F. Lange, Chemical Solution Routes to Single-Crystal Thin Films, *Science,* 1996, **273,** p 903-909
2. C.G. Levi, Metastability and Microstructure Evolution in the Synthesis of Inorganics From Precursors, *Acta. Mater.,* 1998, **46,** p 787-800
3. M. Boulos, Thermal Spray-Materials Synthesis by Thermal Spraying, *Symposium K, MRS Fall Meeting,* November 29-30, 1999 (Boston, MA) p 235-240
4. M. Boulos and E. Pfender, Materials Processing with Thermal Plasmas, *MRS Bull.*, 1996, **21**(8), 65-68
5. C. Delbos, J. Fazilleau, J.F. Coudert, P. Fauchais, L. Bianchi, and K. Wittmann-Teneze, Plasma Spray Elaboration of Finely Structured YSZ Thin Coating by Liquid Suspension Injection, *Thermal Spray 2003: Advancing the Science and Applying the Technology,* B.R. Marple and C. Moreau, Ed., May 5-8, 2003 (Orlando, FL), ASM International, 2003, p 661-669
6. C. Monterrubio-Badillo, H. Ageorges, T. Chartier, J.F. Coudert, and P. Fauchais, Preparation of $LaMnO_3$ Perovskite Thin Films by Suspension Plasma Spraying for SOFC Cathodes, *Surf. Coat. Technol.,* 2006, **200,** p 3743-3756
7. J. Karthikeyan, C.C. Berndt, J. Tikkanen, S. Reddy, and H. Herman, Plasma Spray Synthesis of Nanomaterial Powders and Deposits, *Mater. Sci. Eng. A,* 1997, **238,** p 275-286
8. J. Karthikeyan, C.C. Berndt, S. Reddy, J.Y. Wang, A.H. King, and H. Herman, Nanomaterial Deposits Formed by DC Plasma Spraying of Liquid Feedstocks, *J. Am. Ceram. Soc.,* 1998, **81,** p 121-128
9. T. Bhatia, A. Ozturk, L. Xie, E.H. Jordan, B.M. Cetegen, M. Gell, X. Ma, and N.P. Padture, Mechanism of Ceramic Coating Deposition in Solution-Precursor Plasma Spray, *J. Mater. Res.,* 2002, **17,** p 2363-2372
10. E.H. Jordan, L. Xie, X. Ma, M. Gell, N.P. Padture, B. Cetegen, A. Ozturk, J. Roth, T.D. Xiao, and P.E.C. Bryant, Superior Thermal Barrier Coatings Using Solution Precursor Plasma Spray, *J. Thermal Spray Technol.,* 2004, **13**(1), p 57-65
11. A. Jadhav, N.P. Padture, F. Wu, E.H. Jordan, M. Gell, Thick Ceramic Thermal Barrier Coatings With High Durability Deposited Using Solution-Precursor Plasma Spray, *Mater. Sci. Eng. A,* 2005, **405,** p 313-320
12. S. Shanmugam, A. Hunt and D. Motley, Thin Films of Advanced Materials Via CCVD, *Am. Ceram. Soc. Bull.,* 2002, p 36-41
13. P.S. Devi, J. Margolis, J.B. Parise, C.P. Grey, S. Sampath, H. Herman, and H.D. Gafney, Single Step Deposition of Eu-Doped Y_2O_3 Phosphor Coatings Through a Precursor Plasma Spraying Technique, *J. Mater. Res.,* 2002, **17,** p 2771-2774
14. P.S. Devi, J. Margolis, H.M. Liu, C.P. Grey, S. Sampath, H. Herman, and J.B. Parise, Yttrium Aluminum Garnet (YAG) Films Through a Precursor Plasma Spraying Technique, *J. Am. Ceram. Soc.,* 2001, **84,** p 1906-1908
15. P.S. Devi, Y. Lee, J. Margolis, J.B. Parise, S. Sampath, H. Herman, and J.C. Hanson, Comparison of Citrate-Nitrate Gel Combustion and Precursor Plasma Spray Processes for the Synthesis of Yttrium Aluminum Garnet, *J. Mater. Res.,* 2002, **17,** p 2846-2851
16. X.Z. Guo, B.G. Ravi, P.S. Devi, J.C. Hanson, J. Margolies, R.J. Gambino, J.B. Parise, and S. Sampath, Synthesis of Yttrium Iron Garnet (YIG) by Citrate Nitrate Gel Combustion and Precursor Plasma Spray Processes, *J. Magn. Magn. Mater.,* 2005, **295,** p 145-154
17. X.Z. Guo, B.G. Ravi, Q.Y. Yan, R.J. Gambino, S. Sampath, J. Margolies, and J.B. Parise, Phase Evolution and Magnetic Properties of Precursor Plasma Sprayed Yttrium Iron Garnet Coatings, *Ceram. Int.,* 2005, **32,** p 61-66
18. A.S. Gandhi and C.G. Levi, Phase Selection in Precursor-Derived Yttrium Aluminum Garnet and Related Al_2O_3-Y_2O_3 Compositions, *J. Mater. Res.,* 2005, **20,** p 1017-1025
19. M.H. Yu, P.S. Devi, L.H. Lewis, S. Sampath, J.B. Parise, and R.J. Gambino, Novel Synthesis and Magnetocaloric Assessment of Functional Oxide Perovskites, *Mater Sci. Eng. B,* 2003, **97,** p 245-250